Clay-clast aggregates: a new structural evidence for seismic sliding?

Sébastien Boutareaud, Dan-Gabriel Calugaru, Rahee Han, Olivier Fabbri, K. Mizoguchi, A. Tsutsumi, T. Shimamoto

Clay-clast aggregates: A new textural evidence for seismic fault sliding?

Sébastien Boutareaud,[1,2] Dan-Gabriel Calugaru,[3] Raehee Han,[4] Olivier Fabbri,[1] Kazuo Mizoguchi,[5] Akito Tsutsumi,[6] and Toshihiko Shimamoto[7]

Received 21 November 2007; revised 18 January 2008; accepted 24 January 2008; published 6 March 2008.

[1] To determine the processes responsible for slip-weakening in clayey gouge zones, rotary-shear experiments were conducted at seismic slip rates (equivalent to 0.9 and 1.3 m/s) at 0.6 MPa normal stress on a natural clayey gouge for saturated and non-saturated initial conditions. The mechanical behavior of the simulated faults shows a reproducible slip-weakening behavior, whatever initial moisture conditions. Examination of gouge obtained at the residual friction stage in saturated and non-saturated initial conditions allows the definition of two types of microstructures: a foliated type reflecting strain localization, and a non-foliated type composed of spherical aggregates. Friction experiments demonstrate that liquid-vapor transition of water within gouge due to frictional heating has a high capacity to explain the formation of spherical aggregates in the first meters of displacement. This result suggests that the occurrence of spherical aggregates in natural clayey fault gouges can constitute a new textural evidence for shallow depth pore water phase transition at seismic slip velocity and consequently for past seismic fault sliding.
Citation: Boutareaud, S., D.-G. Calugaru, R. Han, O. Fabbri, K. Mizoguchi, A. Tsutsumi, and T. Shimamoto (2008), Clay-clast aggregates: A new textural evidence for seismic fault sliding?, *Geophys. Res. Lett.*, *35*, L05302, doi:10.1029/2007GL032554.

1. Introduction

[2] Exposures of active faults show that in the upper crust co-seismic slip occurs within a few mm-thick clayey layer called the seismic slip zone thought to exist down to depths of about 5 to 8 km [*Sibson*, 2003]. This slip zone is partly composed of phyllosilicates resulting from rock cataclasis and hydrothermal alteration. Observations and laboratory experiments show that thermo-poro-mechanical properties of this slip zone significantly influence the dynamic frictional strength of active faults by controlling the efficiency of slip-weakening mechanisms during earthquakes [*Rice*, 2006].

[3] Based on theoretical or experimental studies and analyses of fossil co-seismic slip zones exposed at the Earth surface, several thermally-activated mechanisms have been proposed to account for the exponential decay in fault strength. Amongst those mechanisms, effect of pore water phase transition on friction has received little attention [*Mizoguchi et al.*, 2007a; *Sulem et al.*, 2007]. Moreover, no experiment has reported any correlation of seismic slip record with this mechanism, and no diagnostic microstructure allows yet recognition of such a mechanism in natural fault rocks.

[4] The aim of this contribution is to describe spherical aggregates obtained in experiments involving natural clayey fault gouges subjected to high slip velocity rotary-shear, and to propose a possible scenario of formation during the frictional slip-weakening.

2. Sample Assembly and Experimental Conditions

[5] The experimental fault is composed of a 24.4 mm diameter granite cylinder cut perpendicularly to the revolution axis in two halves that are ground to obtain rough wall surfaces, and re-assembled with an intervening layer of ca. 0.8 mm-thick clayey gouge (Figure 1). The assembly is then placed in the testing apparatus where one cylinder remains stationary while the other rotates [*Mizoguchi et al.*, 2007b]. A Teflon ring surrounds the fault in order to avoid gouge expulsion during rotation. The experimental gouge was prepared by sieving a natural clayey gouge from the Usukidani fault, an active fault of SW Japan [*Boutareaud et al.*, 2008]. XRD analyses of the obtained granular material show that it is composed of quartz, K-feldspar, plagioclase, calcite, kaolinite, and illite-smectite mixed-layers. This natural gouge was disaggregated, oven dried at 80°C for several days and then sieved in order to eliminate clasts larger than 80 μm to produce an experimental gouge free from any preferred orientation, with a clay fraction representing 15.7%. Gouge microscope observation shows angular-to-subangular monomineralic and polymineralic clasts which do not constitute aggregated structure. Before each experiment, the sample assembly is consolidated for several hours under the same normal stress as during the experiment (0.6 MPa).

[6] Fourteen representative experiments were carried out at room temperature (20°C) at two fixed rotation rates of 1000 and 1500 rotations per minute corresponding to equivalent slip velocities (V_{eq}) of 0.9 m/s and 1.3 m/s, respectively [see *Hirose and Shimamoto*, 2005]. For each of the two V_{eq}, we conducted two series of experiments, one

[1]Department of Geosciences, University of Franche-Comte, Besançon, France.
[2]Now at Laboratoire de Geophysique Interne et Tectonophysique, CNRS, University of Joseph Fourier, Grenoble, France.
[3]Department of Mathematics, University of Franche-Comte, Besançon, France.
[4]Department of Earth and Environmental Sciences, Korea University, Seoul, Korea.
[5]Earthquake Research Department, National Research Institute for Science and Disaster Prevention, Tsukuba, Japan.
[6]Department of Geology and Mineralogy, Division of Earth and Planetary Sciences, Kyoto University, Kyoto, Japan.
[7]Department of Earth and Planetary Systems Science, Hiroshima University, Higashi-Hiroshima, Japan.

0094-8276/08/2007GL032554

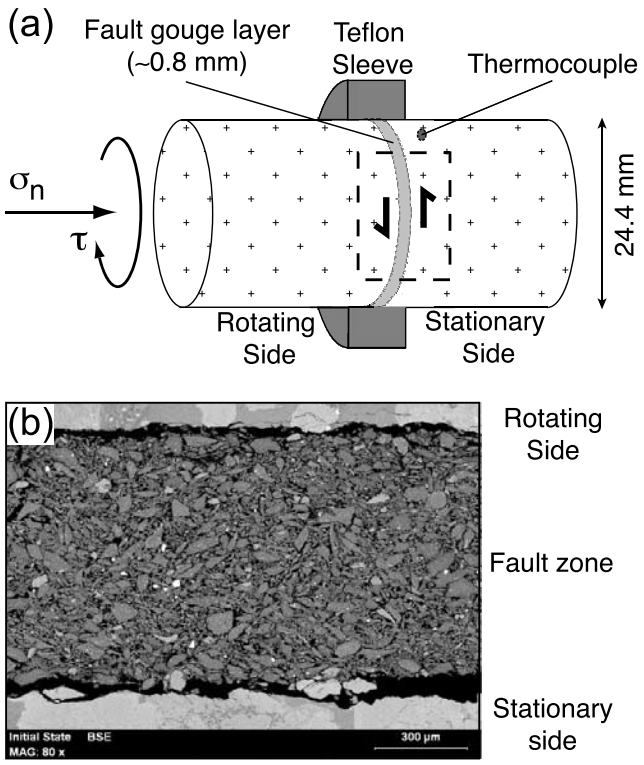

Figure 1. (a) Experimental assembly showing the position of the thin section with respect to the sample assembly. (b) Photomicrograph of the initial gouge.

under non-saturated conditions, that is at room moisture conditions (60% relative humidity) and the other under saturated conditions by using a gouge saturated with distilled water (i.e. the volume of added water is equal to initial gouge pore volume). Measurements of initial gouge porosity were made by dividing the void volume, i.e., the total sample volume minus the granular material volume, by the total sample volume. The applied normal stress was fixed at 0.6 ± 0.2 MPa. The coefficient of dynamic friction μ_d is defined as the ratio of calculated shear stress from the torque to measured normal stress. The maximum thermal expansion of the two granite cylinders along the revolution axis has been calculated to be negligible compared to the measured axial displacement of the sample assembly. Therefore, positive or negative value of the measured axial displacement reflects either gouge compaction or dilatancy, respectively. During the experiments, a thermocouple located on the stationary side and set on the external surface allows a direct temperature measurement at 6.7 mm from the granite-gouge interface (Figure 1).

3. Evolution of Physical Parameters During the Experiments

[7] All experiments are reproducible and show a significant decrease of μ_d from a peak value μ_p down to a steady-state value μ_{ss} (Figure 2). The μ_d value falls below one-third of its initial peak value for total displacements comprised between 10 and 20 m. Second-order oscillations are also observed and could reflect a slight misalignment of the two facing granite cylinders or stick-slip behavior.

[8] For all experiments, the measured axial displacement first consists of a dilatancy comprised between 0.05 mm and 0.2 mm, i.e., a 7 to 29% volume dilation of the gouge layer. This dilatancy reaches a maximum value for displacements comprised between 10 and 20 m, and is then followed by a compaction of about the same order of magnitude. For the 1.3 m/s experiments, two large peaks in axial displacement corresponding to two drops in μ_d were observed at 6.7 m and 7.9 m for experiment #569, and at 0.9 and 6.7 m for experiment #581, in saturated or non-saturated conditions, respectively (Figure 2).

[9] In order to evaluate temperature rise during the experiments, the temperature evolution in a section of granite-gouge assembly has been computed in a 2-D framework by extending the 1-D heat equation of the *Lachenbruch*'s [1980] model. Thus, all frictional work is assumed to convert into heat and temperature changes are only caused

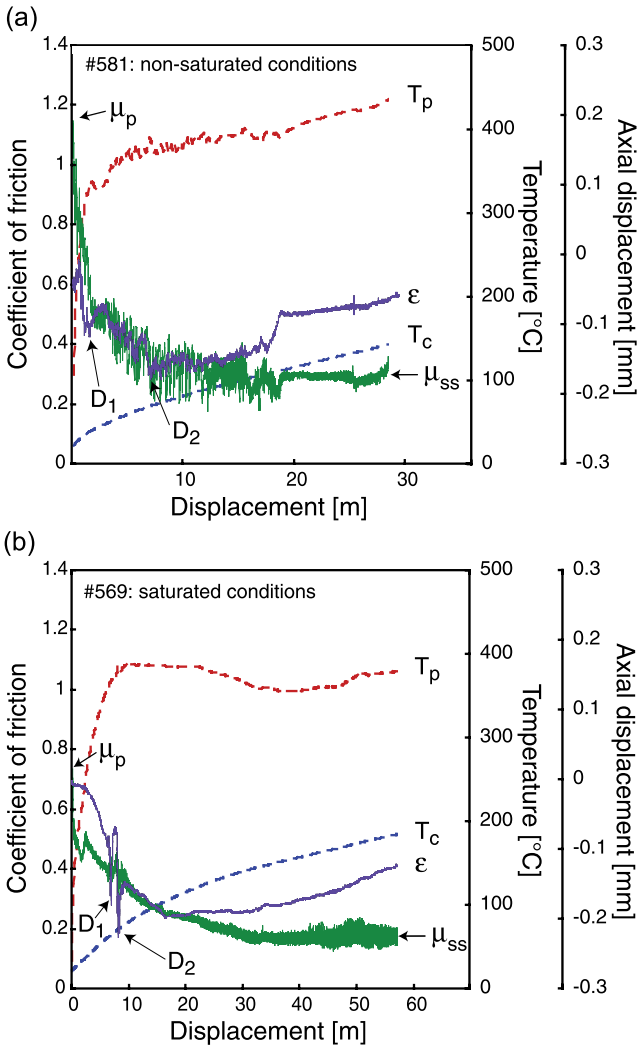

Figure 2. Variations of the friction coefficient (μ_d), the axial displacement (ε), and the temperature calculated at the center (revolution axis, T_c) and at the periphery (T_p) in function of the displacement, for two representative experiments done at V_{eq} = 1.3 m/s. The initial peak friction coefficient is μ_p, and the steady-state friction coefficient is μ_{ss}. *D* stands for a peak event in axial displacement.

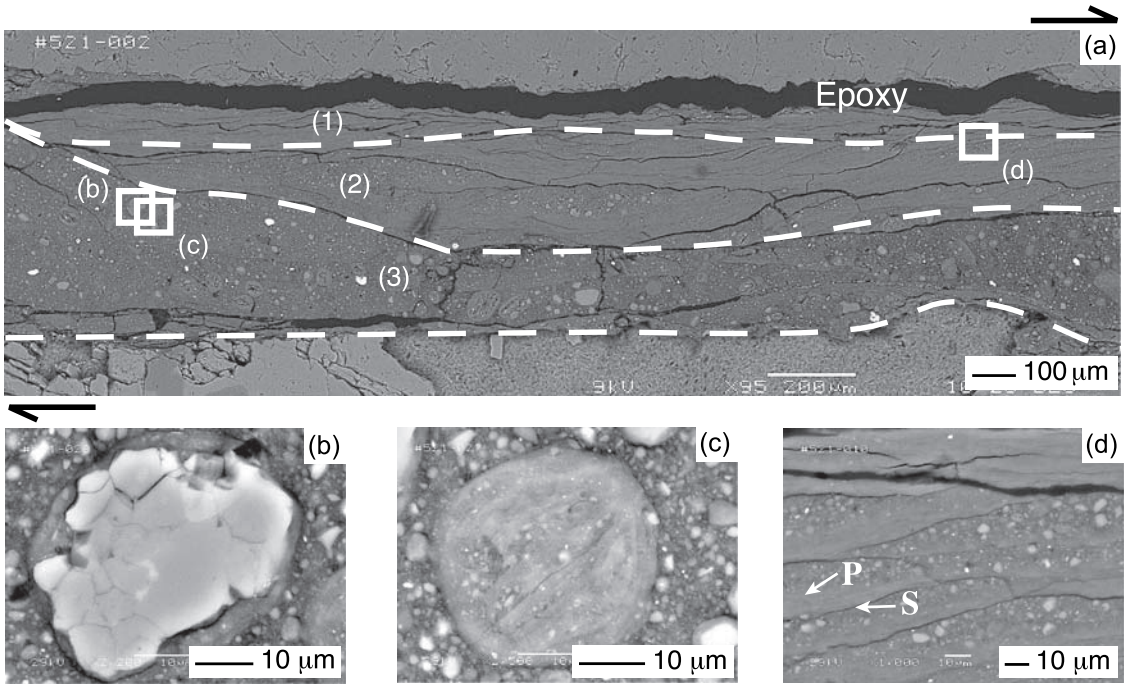

Figure 3. SEM photomicrographs of gouge sheared at V_{eq} = 0.9 m/s in saturated conditions, showing typical characteristics of the two types of microstructures. (a) View of a part of the fault zone showing, from top (rotating side) to bottom (stationary side), a first layer (1) of foliated gouge, a second layer (2) of anastomosed foliated and non-foliated gouges, the third layer (3) being composed only of non-foliated gouge. (b) Example of a clay-clast aggregate with a quartz central clast. (c) Example of a clay-clast aggregate with a central foliated clay-clast derived from the foliated gouge. (d) Anastomosed foliated and non-foliated gouges showing progressive (P) or sharp (S) transitions from one type to the other.

by heat production and heat diffusion. The heat source term is not null only in the "deformation zone" (a narrow layer of constant thickness in the gouge) and is proportional to the shear stress and to the radial position. The SETMP software has been used to solve the heat equation by finite element method [*Calugaru et al.*, 2003] and the numerical modelling has been validated [*Boutareaud*, 2007] by comparing the thermocouple measurements for experiment #569 with the corresponding computed temperature (a maximum difference of 10°C has been observed). The computed temperature evolution is shown in Figure 2 for two points located in the middle of the deformation zone: one at the center of the cylinder (T_c) and the other at the periphery of the cylinder (T_p). For all experiments simulated using this numerical model, the computed temperature increases exponentially and T_p reaches a maximum value comprised between 380 and 520°C at the steady-state friction stage [*Boutareaud*, 2007].

4. Resulting Microstructures

[10] The experiments were stopped once the steady-state friction was reached. Thin sections therefore correspond to a cumulated deformation. Whatever initial moisture conditions, all sections show two types of deformed gouges: non-foliated and foliated (Figure 3).

[11] The non-foliated gouge is a random-fabric clay matrix including rounded to sub-rounded clasts of quartz, feldspar or calcite. A striking characteristic of most clasts (>90%) is that they are surrounded by a cortex of concentric clay layers commonly including very fine (<5 μm) mineral fragments, thus constituting clay-clast aggregates (CCA hereafter; Figure 3). Most of the central clasts are not or moderately fractured and consist of quartz, feldspar or calcite. A small proportion of them are constituted by clay particles with a strong preferred orientation and small (about 1 μm) predominantly rounded to sub-rounded mineral fragments (Figure 3c). The central clasts have diameters as large as 80 μm for the monomineralic clasts, and up to 250 μm for the foliated clasts. In most cases, the cortex remains thinner than 15 μm. In some cases, the aggregates consist only of these concentric clay layers up to 50 μm thick, although they could correspond to off-center sections. Microprobe analysis indicates that the cortex has the same chemical composition as the surrounding gouge. The foliated gouge is composed of clay particles showing a strong preferred orientation parallel to the fault gouge boundaries and rounded clasts whose diameter is smaller than 1 μm. Microprobe analyses indicate that the foliated gouge and the cortex around CCA have the same chemical composition as the non-foliated gouge. No CCA are observed in the foliated gouge.

[12] In the post-experiment fault zones, the distribution of the two types of gouges is not random. The foliated gouge is observed along one or both granite-gouge boundaries. Generally, the foliated gouge is thicker on the rotating side than on the stationary side. The foliated gouge is not always restricted along the granite-gouge boundaries but can also form narrow anastomosed zones, which in some cases cross obliquely the entire fault zone (Figure 3). The non-foliated gouge is distributed in the remaining space. A progressive

transition from the non-foliated to the foliated gouge by decreasing clast-size and increasing clay particle alignment is commonly observed along one or both sides of the oblique narrow foliated gouge zones (Figure 3d).

5. Discussion and Conclusions

[13] From the relationship between the two gouge types, we conclude that the foliated gouge was formed at the expense of the non-foliated type, by progressive comminution and clay particle reorientation. This process has been reported from several friction experiments and natural fault gouges [*Logan et al.*, 1979; *Arch et al.*, 1988; *Chester et al.*, 1993; *Vannucchi et al.*, 2003] and is typically reflecting strain localization. This should occur from the very early stage of the slip as evidenced by previous low-velocity [*Marone*, 1998] and high-velocity [*Mizoguchi*, 2004] gouge friction experiments for small displacements. However, the presence of foliated gouge fragments forming the core of some of the CCA suggests that the foliated gouge can be reworked in the non-foliated gouge, hence showing that at least for some displacement, both gouge types were being simultaneously formed in the fault zone.

[14] Thin section observation shows that the starting natural gouge does not contain any CCA. These were therefore formed during the experimental shear. The nearly perfect sphere-shape and the large size of some inner cores of CCA suggest that they were packed loosely enough and dispersed during shearing to avoid intense grain contact regime and consecutive comminution. The negative axial displacement recorded during the first part of the experiments (Figure 2) validates this assumption showing that the fault zone experienced dilatancy, which provided additional space for grain rolling. The subsequent recorded compaction could correspond to a stage during which no more CCA could be formed due to lack of space. During this second stage, shear deformation was likely accommodated essentially along the foliated-type gouge zones.

[15] Several non-dilatant weakening mechanisms have been recently validated by laboratory experiments, such as frictional melting [*Hirose and Shimamoto*, 2005], silica gel production [*Di Toro et al.*, 2004] and thermal decomposition of carbonates [*Han et al.*, 2007a, 2007b]. However, in the absence of any strong evidence for amorphous material or decomposition products in our experimental products from XRD and microprobe analyses, and considering the observed dilation in axial displacement in the early ten meters, none of these mechanisms appears to be the cause of the weakening in friction. Therefore, another weakening mechanism should be considered. Due to frictional heating, the temperature within the fault zone increases rapidly in the first meters of displacement (Figure 2). According to the water phase diagram [*Roedder and Bodnar*, 1980], the liquid-vapor transition temperature for water at 0.6 MPa is 180°C. It involves a density change from 0.88 to less than 0.1. This implies an increase of the initial water volume by a factor of 10, which corresponds to an expected maximum increase in axial displacement of 5.5 mm. Temperature calculation shows that T_p reached 180°C after less than 0.5 m of displacement against 30 to 60 m (depending on slip velocity) for T_c. This latter sliding distance is larger than that of the observed peak events in axial displacement (Figure 2), which indicates that frictional heating at the periphery of the assembly was sufficient to allow locally first a rapid water liquid-vapor transition, and second gas pressure to briefly exceed the axial normal stress. In the absence of a ring between Teflon and granite cylinder, considering the very high hydraulic diffusivity along the fault plane, gas pressure could not be tightly maintained. This consideration is consistent with the maximum axial displacement measured of 0.2 mm, and with the observed released of water vapor monitored by *Brantut et al.* [2007] during similar non-saturated friction experiments. Then, the shift from dilatancy to compaction observed for a displacement comprised between 10 and 20 m (Figure 2) could be linked with a transition between two stages: first a period during which the production rate of vapor is higher than the radial leaking-diffusion rate across the fault zone, second a period during which the production rate of vapor is lower than the radial leaking-diffusion rate. In addition, the relative high humidity that composed the non-saturated gouge and the related high dilatancy amplitude can be explained by the well-known instantaneous re-hydration of the illite-smectite mixed-layers during sample assembly at high room moisture conditions [*Ferrage et al.*, 2005]. Therefore, the higher amplitude peak events in axial displacement for saturated gouge (D_1 and D_2 on Figure 2b) compared to non-saturated gouge (D_1 and D_2 on Figure 2a) could be directly related to the larger amount of water available that is vaporized, leading to a higher pressurization efficiency.

[16] Spherical aggregates have already been reported from natural rocks including gouge from a seismogenic fault [*Warr and Cox*, 2001], landslide sole [*Beutner and Gerbi*, 2005], or pyroclastic flow sole (with accretionary lapilli) for which core-type and rim-type aggregates with the multiple concentric clay layers containing μm-thick mineral fragments [*Schumacher and Schmincke*, 1995] exhibit similar structural characteristics to the CCA. This suggests that, similarly to the formation of accretionary lapilli, CCA generation should be controlled by a complex interplay of physical and chemical processes [*Gilbert and Lane*, 1994], with electrostatic forces that attract extremely fine mineral fragments from surrounding gouge matrix, and capillary forces of thin liquid bridges on the clast surface that bind fragments to the core of the growing aggregate. Such an aggregation process implies frequent collisions of liquid-coated particles in a turbulent mixture of solid particles and a critical reactive liquid-vapor water [*Beutner and Gerbi*, 2005]. This indicates first that the fault gouge experienced fluidization during shearing, and second that regardless of initial moisture conditions the water content during shearing was close to 5–25% [*Schumacher and Schmincke*, 1995] to provide core surface to be coated with thin condensed liquid water layers [*Gilbert and Lane*, 1994]. The dilatancy observed during experiments is consistent with such a spatial dynamic re-organization of gouge material. The 15 μm-thick maximum thickness of the CCA cortex observed for non-saturated and saturated conditions indicates an equivalent liquid film volume surrounding initial cores whatever initial moisture conditions, which agrees with a comparable amount of liquid-vapor water available within fault gouge during fluidization.

[17] In the seismogenic zone, the pressure-temperature conditions of the water liquid-vapor phase transition will depend on the amount of CO_2 dissolved in water [*Takenouchi and Kennedy*, 1964]. This suggests that the significant decrease in friction we observed experimentally at 0.6 MPa could occur at the seismogenic depth [*Mizoguchi et al.*, 2007a]. Therefore, the occurrence of clay-clast aggregates in crustal clayey fault gouges can be interpreted as a new textural evidence for pore liquid-vapor phase transition of water at seismic slip velocity and consequently for past seismic fault sliding.

[18] **Acknowledgments.** This research was funded by a French-Japanese Doctoral College scholarship to S. B. and INSU grants (DyETI program) to O. F. Frictional experiments were performed at Kyoto University. A. M. Boullier, K. Mair, B. Lanson, and P. Goncalves are sincerely thanked for great help at various stages of the research. G. Di Toro and an anonymous reviewer helped us to greatly improve the manuscript.

References

Arch, J., A. J. Maltman, and R. J. Knipe (1988), Shear-zone geometries in experimentally deformed clays: The influence of water content, strain rate and primary fabric, *J. Struct. Geol.*, *10*, 91–99.

Beutner, E. C., and G. P. Gerbi (2005), Catastrophic emplacement of the Heart Mountain block slide, Wyoming and Montana, USA, *Geol. Soc. Am. Bull.*, *117*, 724–735.

Boutareaud, S. (2007), Slip-weakening mechanisms at high slip-velocities: Insights from analogue and numerical modellings, Ph.D. thesis, 194 pp., Univ. of Fr. Comté, Besançon.

Boutareaud, S., C. A. J. Wibberley, O. Fabbri, and T. Shimamoto (2008), Permeability structure and co-seismic thermal pressurization on fault branches: Insights from the Usukidani Fault, Japan, in *The Internal Structure of Fault Zones: Mechanical and Fluid Flow Properties*, edited by C. A. J. Wibberley et al., *Spec. Publ. Geol. Soc. London*, *299*, in press.

Brantut, N., A. Schubnel, F. Brunet, Y. Leroy, and T. Shimamoto (2007), High velocity frictional properties of pure kaolinite and natural kaolinite-bearing fault gouges, *Geophys. Res. Abstr.*, *8*, Abstract 00927.

Calugaru, D.-G., J. M. Crolet, A. Chambaudet, C. I. Calugaru, and F. Jacob (2003), Inverse problems for flow and transport in the framework of seismic research, *Cah. Phys.*, *XIV*, 9–24.

Chester, F. M., J. P. Evans, and R. Biegel (1993), Internal structure and weakening mechanisms of the San Andreas fault, *J. Geophys. Res.*, *98*, 771–786.

Di Toro, G., D. L. Goldsby, and T. E. Tullis (2004), Friction falls towards zero in quartz rock as slip velocity approaches seismic rates, *Nature*, *427*, 436–439.

Ferrage, E., B. Lanson, B. A. Sakharov, and V. A. Drits (2005), Investigation of smectite hydration properties by modeling experimental X-ray diffraction patterns: Part I. Montmorillonite hydration properties, *Am. Mineral.*, *90*, 1358–1374.

Gilbert, J. S., and S. J. Lane (1994), The origin of accretionary lapilli, *Bull. Volcanol.*, *56*, 398–411.

Han, R., T. Shimamoto, T. Hirose, J. H. Ree, and J. Ando (2007a), Ultralow friction of carbonate faults caused by thermal decomposition, *Science*, *316*, 878–881.

Han, R., T. Shimamoto, J. Ando, and J. H. Ree (2007b), Seismic slip record in carbonate-bearing fault zones: An insight from high-velocity friction experiments on siderite gouge, *Geology*, *35*, 1131–1134.

Hirose, T., and T. Shimamoto (2005), Growth of molten zone as a mechanism of slip weakening of simulated faults in gabbro during frictional melting, *J. Geophys. Res.*, *110*, B05202, doi:10.1029/2004JB003207.

Lachenbruch, A. H. (1980), Frictional heating, fluid pressure, and the resistance to fault motion, *J. Geophys. Res.*, *85*, 6097–6112.

Logan, J. M., M. Friedman, N. Higgs, C. Dengo, and T. Shimamoto (1979), Experimental studies of simulated gouges and their application to studies of natural fault zones, *U. S. Geol. Surv. Open File Rep.*, *79-1239*, 305–343.

Marone, C. (1998), Laboratory-derived friction laws and their application to seismic faulting, *Annu. Rev. Earth Planet. Sci.*, *26*, 643–696.

Mizoguchi, K. (2004), High-velocity frictional behaviour of Nojima fault gouge and its implications for seismogenic fault motion, Ph.D. thesis, 80 pp., Univ. of Kyoto, Kyoto, Jpn.

Mizoguchi, K., M. Takahashi, K. Masuda, and E. Fukuyama (2007a), Fault strength drop due to phase transitions in the pore fluid, *Geophys. Res. Lett.*, *34*, L09313, doi:10.1029/2007GL029345.

Mizoguchi, K., T. Hirose, T. Shimamoto, and E. Fukuyama (2007b), Reconstruction of seismic faulting by high-velocity friction experiments: An example of the 1995 Kobe earthquake, *Geophys. Res. Lett.*, *34*, L01308, doi:10.1029/2006GL027931.

Rice, J. R. (2006), Heating and weakening of faults during earthquake slip, *J. Geophys. Res.*, *111*, B05311, doi:10.1029/2005JB004006.

Roedder, E., and R. J. Bodnar (1980), Geologic pressure determinations from fluid inclusion studies, *Annu. Rev. Earth Planet. Sci.*, *8*, 263–301.

Schumacher, R., and H. U. Schmincke (1995), Models for the origin of accretionary lapilli, *Bull. Volcanol.*, *56*, 626–639.

Sibson, R. H. (2003), Thickness of the seismic slip zone, *Bull. Seismol. Soc. Am.*, *93*, 1169–1178.

Sulem, J., P. Lazar, and I. Vardoulakis (2007), Thermo-poro-mechanical properties of clayey gouge and application to rapid fault shearing, *Int. J. Numer. Anal. Methods Geomech.*, *31*, 523–735.

Takenouchi, S., and G. C. Kennedy (1964), Fluid inclusion gas composition of some mineral deposits and geothermal area, *J. Geochem. Explor.*, *42*, 107–132.

Vannucchi, P., A. Maltman, G. Bettelli, and B. Clennell (2003), On the nature of scaly fabric and scaly clay, *J. Struct. Geol.*, *25*, 673–688.

Warr, L. N., and S. J. Cox (2001), Clay mineral transformations and weakening mechanisms along the Alpine Fault, New Zealand, in *The Nature and Significance of Fault Zone Weakening*, edited by R. E. Holdsworth et al., *Spec. Publ. Geol. Soc. London*, *186*, 85–101.

S. Boutareaud, Laboratoire de Geophysique Interne et Tectonophysique, CNRS, University of Joseph Fourier, BP 53, F-38041 Grenoble cedex, France. (sebastien.boutareaud@ujf-grenoble.fr)

D.-G. Calugaru, Department of Mathematics, University of Franche-Comte, F-25030 Besançon cedex, France.

O. Fabbri, Department of Geosciences, University of Franche-Comte, F-25030 Besançon cedex, France.

R. Han, Department of Earth and Environmental Sciences, Korea University, Seoul 136-701, Korea.

K. Mizoguchi, Earthquake Research Department, National Research Institute for Science and Disaster Prevention, Tsukuba 305-0006, Japan.

T. Shimamoto, Department of Earth and Planetary Systems Science, Hiroshima University, Higashi-Hiroshima 739-8526, Japan.

A. Tsutsumi, Department of Geology and Mineralogy, Division of Earth and Planetary Sciences, Kyoto University 606-8502, Kyoto, Japan.